

Crossover in the local density of states of mesoscopic superconductor/normal-metal/superconductor junctions

Alex Levchenko

School of Physics and Astronomy, University of Minnesota, Minneapolis, MN, 55455, USA

(Dated: May 5, 2008)

Andreev levels deplete energy states above the superconductive gap, which leads to the peculiar non-monotonous crossover in the local density of states of mesoscopic superconductor/normal-metal/superconductor junctions. This effect is especially pronounced in the case when the normal metal bridge length L is small compared to the superconductive coherence length ξ . Remarkable property of the crossover function is that it vanishes not only at the proximity induced gap ϵ_g but also at the superconductive gap Δ . Analytical expressions for the density of states at the both gap edges, as well as general structure of the crossover are discussed.

PACS numbers: 74.45.+c

Experimental advances in probing systems at the mesoscopic scale^{1,2,3,4,5} revived interest to the proximity related problems in superconductor – normal metal (SN) heterostructures.⁶ The most simple physical quantity reflecting proximity effect is the local density of states (LDOS) $\rho(\epsilon, \mathbf{r})$, which can be measured in any spatial point \mathbf{r} at given energy ϵ using scanning tunneling microscopy. The effects of superconductive correlations on the spectrum of a normal metal are especially dramatic in restricted geometries. For example, in the case of superconductor–normal metal–superconductor (SNS) junction, proximity effect induces an energy gap ϵ_g in excitation spectrum of a normal metal with the square root singularity $\rho(\epsilon, \mathbf{r}) \propto \sqrt{\epsilon/\epsilon_g - 1}$ in the density of states just above the threshold $\epsilon - \epsilon_g \ll \epsilon_g$ Ref. 7,8,9,10,11,12 (here and in what follows, ρ will be measured in units of the bare normal metal density of states ν at Fermi energy). The most recent theoretical interest was devoted either to *mesoscopic*^{13,14,16,17} or *quantum*^{18,19,20,21} fluctuation effects on top of mean–field results^{7,8,9,10,11,12} that smear hard gap below ϵ_g and lead to the so called *subgap tail states* with nonvanishing $\rho \propto \exp[-g(1 - \epsilon/\epsilon_g)^{(6-d)/4}]$ at $\epsilon_g - \epsilon \lesssim \epsilon_g$, where g is the dimensionless normal wire conductance and d is the effective system dimensionality. The latter is essentially a nonperturbative result that requires instantonlike approach within σ -model^{19,20} or relies on methods of random matrix theory.^{16,18} Surprisingly, after all of these advances, there is something interesting to discuss about proximity induced properties of the SNS junctions even at the level of quasiclassical approximation by employing Usadel equations.²² The purpose of this work is to point out a subtle feature of the crossover in the local density of states of mesoscopic SNS junctions. The latter was seen in some early and recent studies,^{8,11,12,14,15} however, neither emphasized nor theoretically addressed.

To this end, consider normal wire (N) of length L and width W located between two superconductive electrodes (S). In what follows, we concentrate on diffusive quasi–one–dimensional geometry and the short wire limit $L \ll \xi$, where $\xi = \sqrt{D_S}/\Delta$ is superconductive coherence length, with D_S as the diffusion coefficient in the superconductor and Δ as the energy gap (hereafter, $\hbar = 1$). The center of the wire is chosen to be at $x = 0$ and boundaries with superconductors at $x = \pm L/2$ correspondingly, where x is the coordinate along the wire.

Under the condition $L \ll \xi$, the proximity effect is es-

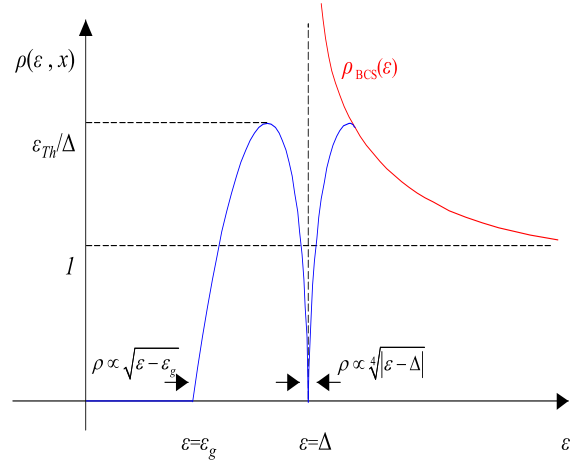


FIG. 1: (Color online) Schematic plot for the local density of states crossover in the short $L \ll \xi$ diffusive SNS junction.

pecially strong — superconductive correlations penetrate the entire volume of the normal region. As the result, the induced energy gap in normal wire ϵ_g is large and turns out to be of the same order as the gap in the superconductor itself $\epsilon_g = \Delta - \delta\Delta$, with the finite size correction $\delta\Delta \sim \Delta^3/\epsilon_{Th}^2 \ll \Delta$, where $\epsilon_{Th} = D_N/L^2$ is the Thouless energy and D_N is the diffusion coefficient in the normal bridge. The latter should be contrasted to the long wire limit $L \gg \xi$, where the proximity effect is weak and the induced gap is $\epsilon_g \sim \epsilon_{Th} \ll \Delta$. Just above the gap $\epsilon - \epsilon_g \ll \epsilon_g$, density of states has square root singularity, which is similar to the $L \gg \xi$ case,^{7,8,9,10,11,12} see Fig. 1, which is a robust property of quasiclassical approximation. However, the prefactor for $L \ll \xi$ is significantly enhanced $\rho(\epsilon, x) \propto (\epsilon_{Th}/\Delta)^2 \sqrt{\epsilon/\epsilon_g - 1}$ (note here that proportionality sign implies characteristic energy dependence, while the exact numerical coefficient is different for a given coordinate x along the wire). The value of ϵ_g is a property of the spectrum, thus it is x independent.

One would naturally expect that above the proximity induced gap ϵ_g , local density of states goes through the maximum $\rho_{\max} = \rho(\epsilon = \Delta, x)$ and then crosses over to the BCS

like DOS $\rho_{BCS} = \epsilon/\sqrt{\epsilon^2 - \Delta^2}$ at $\epsilon > \Delta$, which finally saturates to unity $\rho \rightarrow 1$ at $\epsilon \rightarrow \infty$. Surprisingly, however, the crossover scenario is different. The density of states indeed reaches the maximum, which occurs at $\epsilon \sim \Delta - \delta\Delta/2$, but then decreases and vanishes to zero at superconductive gap Δ with quartic power law behavior $\rho(\epsilon, x) \propto (\epsilon_{Th}/\Delta)^{3/2} \sqrt[4]{|\epsilon/\Delta - 1|}$ for $|\epsilon - \Delta| \lesssim \delta\Delta$. Finally, $\rho(\epsilon, x)$ grows back for $\epsilon > \Delta$ and at the energy scale $\epsilon^* \sim \Delta + \delta\Delta$ crosses over to the ρ_{BCS} . Indeed, observe that $\rho_{BCS}(\epsilon^*) \sim \epsilon_{Th}/\Delta \sim \rho(\epsilon^*, x)$, see Fig. 1. It is important to mention here that the discussed feature appears only at the level of *local* density of states. Energy dependence of the *global* density of states, which is integrated over the entire volume, does not show dip at $\epsilon = \Delta$ (this point will be discussed later in the text).

It seems that crossover picture presented in the Fig. 1 was already numerically seen in previous studies,^{11,12,14,15} however the origin of the soft gap at $\epsilon = \Delta$ was never addressed. One should also note that numerics was performed always for the not too short junctions $L \gtrsim \xi$. It is certainly unusual to find zero in the density of states at the gap edge Δ . In order to get some insight into this bizarre feature, let us consider a *toy model*, which crudely mimics the system under consideration and gives some hints for qualitative understanding. Quantitative theory of the outlined crossover will be developed following this discussion.

Imagine chaotic quantum dot (QD) sandwiched between two superconductors. A quantum dot is really a zero dimensional system, in the sense that $L/\xi \rightarrow 0$ (or equivalently, $\Delta/\epsilon_{Th} \rightarrow 0$). However, one will momentarily see that finite tunneling rate into the dot Γ plays an effective role of Thouless energy ϵ_{Th} . By following Ref. 23 one may construct scattering states and determine quasiparticles excitation spectrum. If in addition we assume that QD supports only one transverse propagating mode, then the discrete spectrum obtained from the poles of the scattering matrix $\mathcal{S}(\epsilon)$ consists of a single nondegenerate Andreev state at energy $\epsilon_o \in [0, \Delta]$, satisfying $\Omega(\epsilon) + \Gamma\epsilon^2 \sqrt{\Delta^2 - \epsilon^2} = 0$, where the function $\Omega(\epsilon)$ is defined by $\Omega(\epsilon) = (\Delta^2 - \epsilon^2)(\epsilon^2 - \Gamma^2/4)$. The density of states in the superconductor–quantum dot–superconductor system is given by $\rho(\epsilon) = \rho_{BCS}(\epsilon) + \delta\rho(\epsilon)$, where

$$\delta\rho(\epsilon) = \frac{1}{2\pi i} \frac{d}{d\epsilon} \ln \left(\frac{\Omega(\epsilon) + i\Gamma\epsilon^2 \sqrt{\epsilon^2 - \Delta^2}}{\Omega(\epsilon) - i\Gamma\epsilon^2 \sqrt{\epsilon^2 - \Delta^2}} \right), \quad (1)$$

which follows from the relation $\rho(\epsilon) = \rho_{BCS} + (1/2\pi i)(d/d\epsilon) \ln \text{Det}\mathcal{S}(\epsilon)$ between DOS and the scattering matrix.²⁴ It is easy to check that in the limit $\Gamma \gg \Delta$ Andreev level is positioned at $\epsilon_o \approx \Delta - 8\Delta^3/\Gamma^2$, which resembles the expression for ϵ_g in the case of the diffusive wire discussed above, where Γ indeed plays the role of Thouless energy. The presence of an Andreev level changes density of states $\rho(\epsilon)$ in two ways. The first contribution $\delta\rho_1(\epsilon)$ originating from $d \ln \text{Det}\mathcal{S}/d\epsilon$ term of Eq. (1) belongs to the subgap part of the spectrum $\epsilon \in [0, \Delta]$ and has structure of the form

$$\delta\rho_1(\epsilon) = \frac{1}{2\pi i} \frac{d}{d\epsilon} \ln \left(\frac{\epsilon - \epsilon_o - i0}{\epsilon - \epsilon_o + i0} \right) = \delta(\epsilon - \epsilon_o), \quad (2)$$

which is nothing else but DOS associated with the single Andreev state. Most interestingly, Andreev level changes $\rho(\epsilon)$

above the superconducting gap as well. Indeed, it follows from the Eq. (1) that at energies $\epsilon > \Delta$ the density of states $\rho(\epsilon)$ gets the correction

$$\delta\rho_2(\epsilon) = -\rho_{BCS}(\epsilon) \frac{\Gamma(2\Delta^2 - \epsilon^2)\Gamma^2/4 - \epsilon^2(\epsilon^2 + \Delta^2)}{\pi(\epsilon^2 - \Delta^2)(\epsilon^2 - \Gamma^2/4)^2 + \Gamma^2\epsilon^4}. \quad (3)$$

Observe that in the immediate vicinity of the superconductive gap $\epsilon - \Delta \lesssim \Delta^3/\Gamma^2$ the correction $\delta\rho_2(\epsilon) \approx -(\Gamma/4\pi\Delta^2)\rho_{BCS}(\epsilon)$ is *negative*, implying that Andreev level *suppresses* bulk superconductive density of states $\rho_{BCS}(\epsilon)$ above the gap. At energy $\epsilon^* \sim \Delta + \Delta^3/\Gamma^2$ the correction given by Eq. (3) reaches its maximum, while ρ_{BCS} is recovered at large energies $\epsilon \gtrsim \Gamma$, where $\delta\rho_2$ decays as $\delta\rho_2(\epsilon) \approx \Gamma/\pi\epsilon^2$. Based on this example, it appears that Andreev level tends to *deplete* bulk BCS density of states at energies $\epsilon - \Delta \lesssim \Delta^3/\Gamma^2$. One should note that the Andreev level leads to pure redistribution of the energy states — there are no additional states above the gap; indeed, $\int_{\Delta}^{\infty} \delta\rho_2(\epsilon)d\epsilon \equiv 0$. If QD supports not only one but a large number of the transverse propagating channels, then cumulative *negative* $\delta\rho_2(\epsilon)$ may compensate $\rho_{BCS}(\epsilon)$, which leads to the vanishing density of states $\rho(\epsilon)$ at the gap edge $\epsilon = \Delta$, see Fig. 1.

Having discussed the qualitative picture of the crossover, let us now turn to the quantitative description. The quasi-classical approach to diffusive SNS structures is based on the Usadel equation²² for the retarded Green's function $\mathcal{G}^R(\mathbf{r}, \epsilon)$. For the latter, we will employ angular parametrization²⁵ $\mathcal{G}^R = \tau_z \cos\theta + \tau_x \sin\theta \cos\phi + \tau_y \sin\theta \sin\phi$, where τ_i is the set of Pauli matrices. In the absence of the phase difference between the S terminals, one can set $\phi \equiv 0$ and Usadel equations for quasi-one-dimension SNS geometry acquires the form

$$\begin{cases} D_N(d^2\theta_N/dx^2) + 2i\epsilon \sin\theta_N = 0 & |x| \leq L/2 \\ D_S(d^2\theta_S/dx^2) + 2i\epsilon \sin\theta_S + 2\Delta \cos\theta_S = 0 & |x| > L/2 \end{cases} \quad (4)$$

where $\theta_{N(S)}(\epsilon, x)$ are the Green's function angles in N(S) parts of the junction, correspondingly. In writing Eq. (4), we assumed step function pair-potential $\Delta(x) = \Delta\eta(|x| - L/2)$, with $\eta(x) = 1$ if $x > 0$ and $\eta(x) = 0$ otherwise. The applicability of this approximation relies on the condition that the width W of the junction is small compared to the coherence length. In this case, nonuniformities in $\Delta(\mathbf{r})$ extend only over the distance of order W from the junction, which is due to the geometrically constrained influence of the narrow junction on the bulk superconductor.²⁶

In the absence of additional tunnel barriers at SN-interfaces, Eqs. (4a) and (4b) are supplemented by the following boundary conditions:²⁷

$$\theta_N(\epsilon, x)|_{x=\pm L/2} = \theta_S(\epsilon, x)|_{x=\pm L/2}, \quad (5a)$$

$$\sigma_N \frac{d\theta_N(\epsilon, x)}{dx} \Big|_{x=\pm L/2} = \sigma_S \frac{d\theta_S(\epsilon, x)}{dx} \Big|_{x=\pm L/2}, \quad (5b)$$

where $\sigma_{N(S)}$ are the conductivities of normal metal and superconductor. Knowing solutions of Usadel equations, one finds local density of states from the general expression

$$\rho(\epsilon, x) = \text{Re}[\cos\theta(\epsilon, x)]. \quad (6)$$

For future convenience, we rotate the Green's function angles as $\theta_N = \pi/2 + i\vartheta_N$ and $\theta_S = \theta_{BCS} + i\vartheta_S$, where $\theta_{BCS} = \pi/2 + i\text{arsinh}\gamma$ with $\gamma = \varepsilon/\sqrt{1-\varepsilon^2}$, and introduce dimensionless variables $\varepsilon = \epsilon/\Delta$, $\lambda = x/L$. After the rotation, Usadel Eq. (4b) for superconducting sides of the junction becomes real and can be easily integrated, providing

$$\vartheta_S(\varepsilon, \lambda) = 4 \operatorname{artanh}\{\exp[-(|\lambda| - 1/2)/\xi_S]\}, \quad (7)$$

where we have introduced the energy depending superconductive coherence length $\xi_S^{-1} = \sqrt{\frac{2\Delta D_N}{\varepsilon_{Th} D_S}} \sqrt[4]{1-\varepsilon^2}$. Equation (4a) may also be exactly solved in terms of elliptic functions; however, this exact solution is not needed for our purposes. Indeed, observe that it follows from the boundary condition [Eq. (5a)] that in the energy range $1 - \varepsilon \ll 1$, the normal metal phase $\operatorname{Re}[\vartheta_N(\varepsilon, \lambda)] \propto \operatorname{arcsinh}\gamma \approx \ln \sqrt{\frac{2}{1-\varepsilon}} \gg 1$ is large everywhere in the N part of the junction. Thus, one may approximate $\sin \theta_N \approx \exp(\vartheta_N)/2$ and solve Eq. (4a) in closed form

$$\vartheta_N(\varepsilon, \lambda) = \vartheta_0(\varepsilon) - \ln[\cosh^2(\lambda/\xi_N)], \quad (8)$$

with normal side coherence length being defined as $\xi_N^{-1} = \sqrt{\frac{2\varepsilon\Delta}{\varepsilon_{Th}}}$ and $\vartheta_0 = \vartheta_N(\varepsilon, 0)$. We now introduce $u_0 = \exp \vartheta_0$ and $u_S = \exp(\operatorname{arcsinh}\gamma + \vartheta_S^B)$, where $\vartheta_S^B = \vartheta_S(\varepsilon, \pm 1/2)$, to rewrite the boundary condition [Eq. (5b)] as

$$u_S/\gamma - 2 = \kappa\gamma(u_0 - u_S), \quad (9)$$

where the interface parameter $\kappa = \sigma_N^2 D_S / \sigma_S^2 D_N$ measures the mismatch of conductivities and diffusion coefficients at the SN boundaries. By using solutions (7) and (8), together with Eq. (9), one eliminates the unknown u_0 and arrives to the algebraic equation for $z = u_S/\gamma - 2$,

$$\mathcal{F}(z, \kappa) = \sqrt{\frac{\gamma\varepsilon\Delta}{8\varepsilon_{Th}}}, \quad (10)$$

where the single parameter $\kappa = \kappa\gamma^2$ scaling function $\mathcal{F}(z, \kappa)$ is given by

$$\mathcal{F}(z, \kappa) = \sqrt{\frac{\kappa}{z + (z+2)\kappa}} \operatorname{arctanh} \sqrt{\frac{z}{z + (z+2)\kappa}}. \quad (11)$$

Knowing the solution of Eq. (10), one finds the density of states at the SN interfaces as

$$\rho(\varepsilon, \pm 1/2) = \frac{\gamma}{2} \operatorname{Im}[z(\varepsilon)]. \quad (12)$$

At the same time, $u_S(\varepsilon)$ together with Eqs. (6)–(8) provide an explicit information about the local density of states $\rho(\varepsilon, x)$ at any position x along the wire.

By looking at Eq. (10), one sees that its right hand side grows to infinity when $\varepsilon \rightarrow 1$, while its left hand side has an absolute maximum for certain value of z . This implies that for all energies below some threshold ε_g , Eq. (10) has the only real solution for z providing $\rho(\varepsilon) \equiv 0$ as it follows from

Eq. (12). The condition $\varepsilon = \varepsilon_g$ when Eq. (10) has a complex solution for z for the first time defines the proximity induced energy gap ε_g . For energies above the gap $\varepsilon > \varepsilon_g$, the density of states is nonzero since $\operatorname{Im}[z] \neq 0$. It turns out that Eq. (10) possesses two qualitatively different solutions depending on the value of the interface parameter κ .

The limit of strong superconductor $\kappa \ll \Delta^2/\varepsilon_{Th}^2$. In this case, $\kappa \ll 1$ and \mathcal{F} function determined by Eq. (11) has the following asymptotes: $\mathcal{F}(z, \kappa) \approx \sqrt{z/4\kappa}$ for $z \ll 1$ and $\mathcal{F}(z, \kappa) \approx \sqrt{\kappa/4z} \ln(2/\kappa)$ for $z \gg 1$. It means that the only relevant z , which determine the maximum of \mathcal{F} are those $z \sim \kappa$. In this region, $\mathcal{F}(z, \kappa)$ may be approximated as $\mathcal{F}(z, \kappa) \approx \sqrt{\frac{\kappa}{z+2\kappa}} \operatorname{arctanh} \sqrt{\frac{z}{z+2\kappa}}$. As a result, the absolute maximum $\mathcal{F}_m = \mathcal{F}(z = z_m)$ occurs at point $z_m \approx 4.5\kappa$, which corresponds to $\mathcal{F}_m \approx 0.5$. Then, the gap determining condition gives

$$\mathcal{F}_m = \sqrt{\frac{\gamma_g \varepsilon_g \Delta}{8\varepsilon_{Th}}} \Rightarrow \varepsilon_g = 1 - \frac{1}{8} \left(\frac{\Delta}{\varepsilon_{Th}} \right)^2, \quad (13)$$

where we have used the notation $\gamma_g = \gamma(\varepsilon_g)$. Just above the gap $\varepsilon - \varepsilon_g \ll \varepsilon_g$, one can expand \mathcal{F} in Taylor series around the maximum $\mathcal{F} \approx \mathcal{F}_m + b(z - z_m)^2$, with $b = (1/2)(d^2\mathcal{F}/dz^2)_{z=z_m}$ to find $z \approx z_m + i\sqrt{\frac{1}{b}} \sqrt{\sqrt{\frac{\gamma\varepsilon\Delta}{8\varepsilon_{Th}}} - \sqrt{\frac{\gamma_g\varepsilon_g\Delta}{8\varepsilon_{Th}}}}$. By using now definition (12), one finds for the density of states just above the proximity induced gap at SN-interface,

$$\rho(\varepsilon, \pm 1/2) \propto \left(\frac{\varepsilon_{Th}}{\Delta} \right)^2 \sqrt{\frac{\varepsilon - \varepsilon_g}{\varepsilon_g}}, \quad \varepsilon - \varepsilon_g \ll \varepsilon_g, \quad (14)$$

where the numerical coefficient of the order of unity was omitted. For the other limiting case, in the vicinity of the superconductive gap $\varepsilon \sim 1$, Eq. (10) is solved by $z \approx -\pi^2 p^2 (1 - 4ip)$ with $p = \sqrt{\frac{\varepsilon_{Th}}{\Delta}} \sqrt[4]{1-\varepsilon}$, which gives for the density of states,

$$\rho(\varepsilon, \pm 1/2) \propto \left(\frac{\varepsilon_{Th}}{\Delta} \right)^{3/2} \sqrt[4]{\frac{|\varepsilon - \Delta|}{\Delta}}, \quad |\varepsilon - \Delta| \lesssim \delta\Delta. \quad (15)$$

This asymptotic result holds above Δ as well. Observe that at $\varepsilon \sim \varepsilon_g + \delta\Delta/2$, Eqs. (14) and (15) crossover to each other, while at $\varepsilon \sim \Delta + \delta\Delta$, Eq. (15) crossovers to the BCS like density of states.

The limit of weak superconductor $\kappa \gg \Delta^2/\varepsilon_{Th}^2$. This limiting case corresponds to the situation when $\kappa \gg 1$ and the expression for \mathcal{F} greatly simplifies $\mathcal{F}(z, \kappa) \approx \sqrt{\frac{1}{\kappa} \frac{\sqrt{z}}{z+2}}$. At $z_m = 2$, the function \mathcal{F} has the maximum $\mathcal{F}_m = \sqrt{1/8\kappa_g}$, were $\kappa_g = \kappa\gamma_g^2$, so that the gap determining condition is different from Eq. (13) and reads

$$\sqrt{\frac{1}{8\kappa_g}} = \sqrt{\frac{\gamma_g \varepsilon_g \Delta}{8\varepsilon_{Th}}} \Rightarrow \varepsilon_g = 1 - \frac{1}{2} \left(\frac{\kappa\Delta}{\varepsilon_{Th}} \right)^{2/3}. \quad (16)$$

To calculate the asymptotes for density of states at both gap edges, one follows the same steps as in the previous case and

finds

$$\rho(\epsilon, \pm 1/2) \propto \left(\frac{\epsilon_{Th}}{\kappa\Delta}\right)^{2/3} \sqrt{\frac{\epsilon - \epsilon_g}{\epsilon_g}}, \quad \epsilon - \epsilon_g \ll \epsilon_g, \quad (17a)$$

$$\rho(\epsilon, \pm 1/2) \propto \sqrt{\frac{\epsilon_{Th}}{\kappa\Delta}}^4 \sqrt{\frac{|\epsilon - \Delta|}{\Delta}}, \quad |\epsilon - \Delta| \lesssim \delta\Delta^*, \quad (17b)$$

where $\delta\Delta^* \sim \Delta(\kappa\Delta/\epsilon_{Th})^{2/3}$. Equations (14), (15) and (17) complement our qualitative considerations presented at the beginning of this paper.

At this point, let us discuss the obtained results and limits of their applicability. (i) We have studied the energy dependence of the local density of states for short ($L \ll \xi$) diffusive SNS junctions. Although $\rho(\epsilon, x)$ was analytically calculated at SN interfaces only it turns out that its energy dependence is generic for any $x \in [-L/2, L/2]$ and given by Eqs. (14), (15) and (17). The exact numerical prefactor, however, is x dependent and should be determined numerically. (ii) Let us stress that the discussed feature in the $\rho(\epsilon, x)$ at $\epsilon \sim \Delta$ disappears at the level of global $\langle\rho(\epsilon)\rangle$, which is integrated over the volume, density of states. Indeed, the spatial

integration brings an additional factor of ξ_S^d , where d is an effective dimensionality of superconductor, which is due to the long spatial tails of Andreev states penetrating deep inside the superconductor [note that because of these tails, it is not correct to integrate $\rho(\epsilon, x)$ over $x \in [-L/2, L/2]$ only]. For quasi-one-dimensional geometry discussed here, a factor of $\xi_S \propto (\frac{1}{1-\epsilon})^{1/4}$ gained after x integration exactly compensates the dip in $\rho(\epsilon, x)$ at $\epsilon \sim \Delta$ [see Eqs. (15) and (17b)], leading to the finite value $\langle\rho(\epsilon=\Delta)\rangle \sim \epsilon_{Th}/\Delta$. For $d > 1$, the density of states at superconductive gap edge $\epsilon \sim \Delta$ should diverge as a certain power-law $\langle\rho(\epsilon)\rangle \sim (\epsilon - \Delta)^{-p}$ for $p > 0$. (iii) It follows from the numerical analysis¹² that presence of additional tunnel barriers at SN interfaces alters soft gap and leads to the nonzero density of states at the gap edge Δ . (iv) Finite superconductive phase ϕ imposed across the junction shifts position of the proximity induced gap⁹ $\epsilon_g(\phi)$, such that $\epsilon_g(\phi = \pi) = 0$, and also changes shape of the crossover function. However, zero in the LDOS at $\epsilon = \Delta$ and asymptotes at both gap edges persist.

Numerous useful discussions with A. Kamenev and L. Glazman, which initiated and stimulated this work are kindly acknowledged. This research is supported by DOE Grant No. 08ER46482.

-
- ¹ S. Guéron, H. Pothier, Norman O. Birge, D. Esteve and M. H. Devoret, Phys. Rev. Lett. **77**, 3025 (1996).
 - ² M. F. Goffman, R. Cron, A. Levy Yeyati, P. Joyez, M. H. Devoret, D. Esteve, and C. Urbina, Phys. Rev. Lett. **85**, 170 (2000).
 - ³ E. Scheer, W. Belzig, Y. Naveh, M. H. Devoret, D. Esteve, and C. Urbina, Phys. Rev. Lett. **86**, 284 (2001).
 - ⁴ A. Anthore, H. Pothier, and D. Esteve, Phys. Rev. Lett. **90**, 127001 (2003).
 - ⁵ Yong-Joo Doh, Jorden A. van Dam, Aarnoud L. Roest, Erik P. A. M. Bakkers, Leo P. Kouwenhoven, Silvano De Franceschi, Science **309**, 272 (2005).
 - ⁶ See, e.g., *Mesoscopic Superconductivity*, edited by P. F. Bagwell special issue of Superlattices Microstruct. **25**, 5–6 (1999).
 - ⁷ A. A. Golubov, E. P. Houwman, J. G. Gijsbertsen, V. M. Krasnov, J. Flokstra, H. Rogalla, and M. Yu. Kupriyanov, Phys. Rev. B **51**, 1073 (1995).
 - ⁸ W. Belzig, C. Bruder, and G. Schön, Phys. Rev. B **54**, 9443 (1996).
 - ⁹ F. Zhou, P. Charlat, B. Spivak, and B. Pannetier, J. Low Temp. Phys. **110**, 841 (1998).
 - ¹⁰ Ya. V. Fominov and M. V. Feigel'man, Phys. Rev. B **63**, 094518 (2001).
 - ¹¹ T. T. Heikkilä, J. Särkkä, and F. K. Wilhelm, Phys. Rev. B **66**, 184513 (2002).
 - ¹² J. C. Hammer, J. C. Cuevas, F. S. Bergeret, and W. Belzig, Phys. Rev. B **76**, 064514 (2007).
 - ¹³ K. M. Frahm, P. W. Brouwer, J. A. Melsen, and C. W. J. Beenakker, Phys. Rev. Lett. **76**, 2981 (1996).
 - ¹⁴ A. Altland, B. D. Simons and D. Taras-Semchuk, Adv. Phys. **49**, 321 (2000).
 - ¹⁵ F. K. Wilhelm and A. A. Golubov, Phys. Rev. B **62**, 5353 (2000).
 - ¹⁶ M. G. Vavilov, P. W. Brouwer, V. Ambegaokar, and C. W. J. Beenakker, Phys. Rev. Lett. **86**, 874 (2001).
 - ¹⁷ J. S. Meyer and B. D. Simons, Phys. Rev. B **64**, 134516 (2001).
 - ¹⁸ M. Titov, N. A. Mortensen, H. Schomerus, and C. W. J. Beenakker, Phys. Rev. B **64**, 134206 (2001).
 - ¹⁹ A. Lamacraft and B. D. Simons, Phys. Rev. Lett. **85**, 4783 (2000).
 - ²⁰ P. M. Ostrovsky, M. A. Skvortsov, and M. V. Feigel'man, Phys. Rev. Lett. **87**, 027002 (2001).
 - ²¹ A. Silva, Phys. Rev. B **72**, 224505 (2005).
 - ²² K. D. Usadel, Phys. Rev. Lett. **25**, 507 (1970).
 - ²³ C. W. J. Beenakker and H. van Houten, *Single-Electron Tunneling and Mesoscopic Devices*, edited by H. Koch and H. Lübbig, Springer, Berlin, (1992), pp. 175-179.
 - ²⁴ E. Akkermans, A. Auerbach, J. E. Avron, and B. Shapiro, Phys. Rev. Lett. **66**, 76 (1991).
 - ²⁵ W. Belzig, F. K. Wilhelm, C. Bruder, G. Schön, and A. D. Zaikin, Superlattices Microstruct. **25**, 1251 (1999).
 - ²⁶ K. K. Likharev, Rev. Mod. Phys. **51**, 101 (1979).
 - ²⁷ M. Yu. Kupriyanov and V. F. Lukichev, Sov. Phys. JETP **67**, 1163 (1988).